J|A|C|S
ARTICLES

Published on Web 09/01/2009

Hydration of Alkaline Earth Metal Dications: Effects of Metal Ion Size Determined Using Infrared Action Spectroscopy

Matthew F. Bush,[†] Jeremy T. O'Brien, James S. Prell, Chih-Che Wu,[§] Richard J. Saykally, and Evan R. Williams*

Department of Chemistry, University of California, Berkeley, California 94720-1460

Received February 9, 2009; E-mail: williams@cchem.berkeley.edu

Abstract: Infrared laser action spectroscopy is used to characterize divalent Mg, Ca, and Ba ions solvated by discrete numbers of water molecules in the gas phase. The spectra of the hexahydrated ions are very similar and indicate that all six water molecules directly solvate the metal ion. The spectra of the heptahydrated ions indicate the presence of populations of structures that have a water molecule in the outer shell for all ions and an average coordination number (CN) for Ba that is higher than that for Ca or Mg. Comparisons between CN values obtained from M06 density functional and local MP2 theory indicate that the B3LYP density functional favors smaller CN values. The spectra of clusters containing at least 12 water molecules indicate that the relative abundance of single-acceptor water molecules for a given cluster size decreases with increasing metal ion size, indicating that tighter water binding to smaller metal ions disrupts the hydrogen bond network and results in fewer net hydrogen bonds. The spectra of the largest clusters ($n = 32$) are very similar, suggesting that intrinsic water properties are more important than ion−water interactions by that size, but subtle effects of Mg on surface water molecules are observed even for such large cluster sizes.

Introduction

The effects of ions on water structure are a delicate balance between ion−water interactions and intrinsic intersolvent hydrogen bonding. Studies of hydrated ions can reveal detailed information about both direct ion−solvent interactions and solvent shell structures. Sequential water binding energies measured by a variety of techniques reveal the thermochemistry of the initial ion solvation process,[1−3] and infrared action spectra can provide detailed structural information.[4−16] Ions also affect solvent properties through indirect interactions with the hydrogen-bond network. Results from studies of increasingly large clusters can be extrapolated to reveal information about the structures and reactivities of ions in solution and near interfaces, including phenomena that have not been measured directly in condensed-phase experiments. For example, photoelectron spectra of sequentially larger hydrated electron clusters have been measured to determine thermodynamic values for electrons in condensed-phase environments,[17] electron recombination energies for solvated metal ion clusters have been used to obtain absolute electrochemical potentials in solution,[18,19] and infrared multiple photon dissociation (IRMPD) action spectra of $H^+(H_2O)_{21}$ have been used as evidence to support structures in which the excess charge is localized at the cluster surface,[20−23]

[†] Current address: Department of Chemistry, University of Cambridge, Cambridge CB2 1EW, UK.

[§] Current address: Department of Applied Chemistry, National Chi Nan University, Puli, Nantou 545, Taiwan.

(1) Peschke, M.; Blades, A. T.; Kebarle, P. *J. Phys. Chem. A* **1998**, *102*, 9978–9985.
(2) Rodriguez-Cruz, S. E.; Jockusch, R. A.; Williams, E. R. *J. Am. Chem. Soc.* **1999**, *121*, 8898–8906.
(3) Carl, D. R.; Moision, R. M.; Armentrout, P. B. *Int. J. Mass Spectrom.* **2007**, *265*, 308–325.
(4) Miller, D. J.; Lisy, J. M. *J. Chem. Phys.* **2006**, *124*, 024319.
(5) Robertson, W. H.; Johnson, M. A. *Annu. Rev. Phys. Chem.* **2003**, *54*, 173–213.
(6) Inokuchi, Y.; Ohshimo, K.; Misaizu, F.; Nishi, N. *J. Phys. Chem. A* **2004**, *108*, 5034–5040.
(7) Walters, R. S.; Pillai, E. D.; Duncan, M. A. *J. Am. Chem. Soc.* **2005**, *127*, 16599–16610.
(8) Bush, M. F.; Saykally, R. J.; Williams, E. R. *ChemPhysChem* **2007**, *8*, 2245–2253.
(9) O'Brien, J. T.; Williams, E. R. *J. Phys. Chem. A* **2008**, *112*, 5893–5901.
(10) Kamariotis, A.; Boyarkin, O. V.; Mercier, S.; Beck, R. D.; Bush, M. F.; Williams, E. R.; Rizzo, T. R. *J. Am. Chem. Soc.* **2006**, *128*, 905–916.
(11) Bush, M. F.; Saykally, R. J.; Williams, E. R. *J. Am. Chem. Soc.* **2007**, *129*, 2220–2221.
(12) Zhou, J.; Santambrogio, G.; Brümmer, M.; Moore, D. T.; Wöste, L.; Meijer, G.; Neumark, D. M.; Asmis, K. R. *J. Chem. Phys.* **2006**, *125*, 111102.
(13) Yeh, L. I.; Okumura, M.; Myers, J. D.; Price, J. M.; Lee, Y. T. *J. Chem. Phys.* **1989**, *91*, 7319–7330.
(14) Carnegie, P. D.; Bandyopadhyay, B.; Duncan, M. A. *J. Phys. Chem. A* **2008**, *112*, 6237–6243.
(15) Choi, J. H.; Kuwata, K. T.; Cao, Y. B.; Okumura, M. *J. Phys. Chem. A* **1998**, *102*, 503–507.
(16) Iino, T.; Ohashi, K.; Inoue, K.; Judai, K.; Nishi, N.; Sekiya, H. *Eur. Phys. J. D* **2007**, *43*, 37–40.
(17) Coe, J. V.; Williams, S. M.; Bowen, K. H. *Int. Rev. Phys. Chem.* **2008**, *27*, 27–51.
(18) Donald, W. A.; Leib, R. D.; O'Brien, J. T.; Bush, M. F.; Williams, E. R. *J. Am. Chem. Soc.* **2008**, *130*, 3371–3381.
(19) Donald, W. A.; Leib, R. D.; O'Brien, J. T.; Williams, E. R. *Chem.—Eur. J.* **2009**, *15*, 5926–5934.
(20) Shin, J. W.; Hammer, N. I.; Diken, E. G.; Johnson, M. A.; Walters, R. S.; Jaeger, T. D.; Duncan, M. A.; Christie, R. A.; Jordan, K. D. *Science* **2004**, *304*, 1137–1140.
(21) Miyazaki, M.; Fujii, A.; Ebata, T.; Mikami, N. *Science* **2004**, *304*, 1134–1137.
(22) Chang, H. C.; Wu, C. C.; Kuo, J. L. *Int. Rev. Phys. Chem.* **2005**, *24*, 553–578.
(23) Iyengar, S. S. *J. Chem. Phys.* **2007**, *126*, 216101.

10.1021/ja901011x CCC: $40.75

which is consistent with condensed-phase experiments that indicate enhanced concentrations of hydrated protons at the air/water interface.[24−26]

IRMPD action spectroscopy is a well-established tool to probe the structures of hydrated clusters of singly charged cations[4,6,7,13,16,20−22,27,28] and anions.[5,15,29] Tremendous advances in characterizing hydrated multiply charged ions have been made in recent years, and spectra have been reported for $Ca^{2+}(H_2O)_n$,[8,30] $Cu^{2+}(H_2O)_n$,[9] $Cr^{2+}(H_2O)$,[14] $M^{3+}(H_2O)_n$ (M = rare earth metal),[31] and $SO_4^{2-}(H_2O)_n$.[11,12] IRMPD spectra of $Cu^{2+}(H_2O)_n$ support a coordination number (CN) of 4 for $n = 6$ and the presence of a third solvent shell for $n \geq 10$.[9] IRMPD spectra of $La^{3+}(H_2O)_n$ over a size range in which the reactivity changes ($n = 17-20$) indicate that the relative abundance of single-acceptor water molecules decreases with n. These results indicate that IRMPD spectra of hydrated multiply charged ions can provide insights into the structures and reactivities of these ions.

The structures of hydrated divalent alkaline earth metal ions in the gas phase have been studied using a variety of experimental and computational methods. Based on comparisons between experimental and calculated water molecule binding energies and trends in the experimental water binding entropies determined using high-pressure mass spectrometry, Kebarle and co-workers reported that the CN values for Mg^{2+} and Ca^{2+} are 6 and that the CN value of Ba^{2+} may be "as high as 8 or 9".[1] Blackbody infrared radiative dissociation (BIRD) experiments indicate that all six water molecules coordinate directly to the metal ion in $M^{2+}(H_2O)_6$ (M = Ca, Sr, and Ba) and that two structural isomers may be present for $Mg^{2+}(H_2O)_6$.[2,32] Although the water binding energy of $Ca^{2+}(H_2O)_7$ was consistent with that calculated for a CN = 6 structure, the monotonic decrease in water binding energy with increasing cluster size suggests a CN = 7 structure,[33] illustrating the difficulty in deducing CN values from water binding energies alone. Results from threshold collision-induced dissociation experiments and theory also indicate a CN = 6 structure for Ca^{2+} clusters with 6−9 water molecules.[3] Many computational studies indicate that the CN values for M = Mg and Ca in $M^{2+}(H_2O)_n$ are 6,[3,8,34−36] although structures with higher CN values can be close in energy for M = Ca.[8,36] Tunell and Lim report that CN = 7 structures are lowest energy for M = Ba in $M^{2+}(H_2O)_n$ ($n \leq 9$).[35] Recent results from IRMPD spectroscopy of $Ca^{2+}(H_2O)_n$ with n up to 69 indicate a change in CN from 6 to 8 for clusters with 12 or more water molecules.[30] Many condensed-phase experiments and simulations support CN values for M = Mg, Ca, and Ba of 6,[37] 7 or 8,[37−48] and 9,[37,49−51] respectively. However, the range of reported CN values from condensed-phase studies is greater than those from gas-phase studies.[30,37] Additionally, recent X-ray absorption spectroscopy experiments on liquid microjets indicate that inner-shell water molecules transfer significant charge to alkaline earth metal cations and that a greater extent of transfer is observed for Mg^{2+} than Ca^{2+}.[52]

Here, IRMPD spectra are reported for selected $Mg^{2+}(H_2O)_n$ and $Ba^{2+}(H_2O)_n$ clusters. These results are compared extensively with those reported previously[8,30] for $Ca^{2+}(H_2O)_n$ to elucidate the effects of alkaline earth metal ion size on cluster structure.

Methods

Experimental Methods. Experiments were performed on a 2.7 T Fourier transform ion cyclotron resonance mass spectrometer.[8,53] $M^{2+}(H_2O)_n$ (M = Mg and Ba) clusters were formed by nanoelectrospray ionization from 1 mM aqueous solutions of $MgSO_4$ and $BaCl_2$, respectively. Ion abundances for the clusters of interest were optimized by adjusting nanoelectrospray interface and trapping conditions.[54] Ions were trapped in a cylindrical ion cell surrounded by a copper jacket, the temperature of which is regulated by a controlled liquid nitrogen flow.[55] The clusters of interest were isolated using a stored waveform inverse Fourier transform pulse and subsequently irradiated with 7−1200 pulses of IR radiation (8−21 mJ per ~6 ns pulse) from a tunable 10 Hz optical parametric oscillator/amplifier (LaserVision, Bellevue, WA). IRMPD spectra were obtained by plotting the power- and time-corrected photodissociation intensity as a function of laser frequency.[53]

Computational Methods. Candidate structures of $Ca^{2+}(H_2O)_n$ were reported previously,[8] and those for $Mg^{2+}(H_2O)_n$ and $Ba^{2+}(H_2O)_n$ were generated by changing the identity of the metal ion in the $Ca^{2+}(H_2O)_n$ structures. Electronic energy-minimized structures and harmonic vibrational frequencies were determined

(24) Petersen, P. B.; Saykally, R. J. *J. Phys. Chem. B* **2005**, *109*, 7976–7980.
(25) Levering, L. M.; Sierra-Hernandez, M. R.; Allen, H. C. *J. Phys. Chem. C* **2007**, *111*, 8814–8826.
(26) Tian, C.; Ji, N.; Waychunas, G. A.; Shen, Y. R. *J. Am. Chem. Soc.* **2008**, *130*, 13033–13039.
(27) Jiang, J. C.; Wang, Y. S.; Chang, H. C.; Lin, S. H.; Lee, Y. T.; Niedner-Schatteburg, G. *J. Am. Chem. Soc.* **2000**, *122*, 1398–1410.
(28) Wu, C. C.; Lin, C. K.; Chang, H. C.; Jiang, J. C.; Kuo, J. L.; Klein, M. L. *J. Chem. Phys.* **2005**, *122*, 074315.
(29) Asmis, K. R.; Santambrogio, G.; Zhou, J.; Garand, E.; Headrick, J.; Goebbert, D.; Johnson, M. A.; Neumark, D. M. *J. Chem. Phys.* **2007**, *126*, 191105.
(30) Bush, M. F.; Saykally, R. J.; Bush, M. F. *J. Am. Chem. Soc.* **2008**, *130*, 15482–15489.
(31) Bush, M. F.; Saykally, R. J.; Williams, E. R. *J. Am. Chem. Soc.* **2008**, *130*, 9122–9128.
(32) Rodriguez-Cruz, S. E.; Jockusch, R. A.; Williams, E. R. *J. Am. Chem. Soc.* **1999**, *121*, 1986–1987.
(33) Rodriguez-Cruz, S. E.; Jockusch, R. A.; Williams, E. R. *J. Am. Chem. Soc.* **1998**, *120*, 5842–5843.
(34) Adrian-Scotto, M.; Mallet, G.; Vasilescu, D. *THEOCHEM* **2005**, *728*, 231–242.
(35) Tunell, I.; Lim, C. *Inorg. Chem.* **2006**, *45*, 4811–4819.
(36) Katz, A. K.; Glusker, J. P.; Beebe, S. A.; Bock, C. W. *J. Am. Chem. Soc.* **1996**, *118*, 5752–5763.
(37) Ohtaki, H.; Radnai, T. *Chem. Rev.* **1993**, *93*, 1157–1204.
(38) Jiao, D.; King, C.; Grossfield, A.; Darden, T. A.; Ren, P. Y. *J. Phys. Chem. B* **2006**, *110*, 18553–18559.
(39) Lightstone, F. C.; Schwegler, E.; Allesch, M.; Gygi, F.; Galli, G. *ChemPhysChem* **2005**, *6*, 1745–1749.
(40) Jalilehvand, F.; Spångberg, D.; Lindqvist-Reis, P.; Hermansson, K.; Persson, I.; Sandström, M. *J. Am. Chem. Soc.* **2001**, *123*, 431–441.
(41) Ikeda, T.; Boero, M.; Terakura, K. *J. Chem. Phys.* **2007**, *127*, 074503.
(42) Tofteberg, T.; Ohrn, A.; Karlstrom, G. *Chem. Phys. Lett.* **2006**, *429*, 436–439.
(43) Naor, M. M.; Van Nostrand, K.; Dellago, C. *Chem. Phys. Lett.* **2003**, *369*, 159–164.
(44) Fulton, J. L.; Heald, S. M.; Badyal, Y. S.; Simonson, J. M. *J. Phys. Chem. A* **2003**, *107*, 4688–4696.
(45) Smirnov, P.; Yamagami, M.; Wakita, H.; Yamaguchi, T. *J. Mol. Liq.* **1997**, *73−74*, 305–316.
(46) Schwenk, C. F.; Loeffler, H. H.; Rode, B. M. *J. Chem. Phys.* **2001**, *115*, 10808–10813.
(47) Badyal, Y. S.; Barnes, A. C.; Cuello, G. J.; Simonson, J. M. *J. Phys. Chem. A* **2004**, *108*, 11819–11827.
(48) Megyes, T.; Grósz, T.; Radnai, T.; Bakó, I.; Pálinkás, G. *J. Phys. Chem. A* **2004**, *108*, 7261–7271.
(49) Hofer, T. S.; Rode, B. M.; Randolf, B. R. *Chem. Phys.* **2005**, *312*, 81–88.
(50) Albright, J. N. *J. Chem. Phys.* **1972**, *56*, 3783–3786.
(51) Dangelo, P.; Pavel, N. V.; Roccatano, D.; Nolting, H. F. *Phys. Rev. B* **1996**, *54*, 12129–12138.
(52) Cappa, C. D.; Smith, J. D.; Messer, B. M.; Cohen, R. C.; Saykally, R. J. *J. Phys. Chem. B* **2006**, *110*, 5301–5309.
(53) Bush, M. F.; O'Brien, J. T.; Prell, J. S.; Saykally, R. J.; Williams, E. R. *J. Am. Chem. Soc.* **2007**, *129*, 1612–1622.
(54) Bush, M. F.; Saykally, R. J.; Williams, E. R. *Int. J. Mass Spectrom.* **2006**, *253*, 256–262.
(55) Wong, R. L.; Paech, K.; Williams, E. R. *Int. J. Mass Spectrom.* **2004**, *232*, 59–66.

using B3LYP/6-311++G(2d,2p) calculations (CRENBL[56] effective core potential (ECP) for Ba). Single-point energies for these geometries were also calculated at the M06 hybrid method density functional[57] and local triatomics-in-molecule second-order Møller–Plesset (TRIM-MP2)[58] levels of theory using the CRENBL ECP for Ba and the 6-311++G(2d,2p) basis set for all remaining elements. All calculations were performed using Q-Chem v.3.1.[59]

Results and Discussion

Infrared Action Spectroscopy. The distributions of $M^{2+}(H_2O)_n$ formed by nanoelectrospray ionization are generally broad and can be shifted to larger or smaller sizes by changing experimental parameters, such as the temperature of the heated metal capillary.[54] For clusters with $n < 12$, a single precursor ion was isolated and photodissociated using methods reported previously for $Ca^{2+}(H_2O)_{4-10}$.[8] Because the binding energy of water is much higher at the smallest cluster sizes,[1,60] higher copper jacket temperatures were used for the smaller clusters to increase their internal energy via interaction with the surrounding blackbody radiation field.[61] For clusters with $n \geq 12$, multiple precursor ions were isolated and photodissociated simultaneously using methods reported previously for $Ca^{2+}(H_2O)_{12-69}$.[30] For the larger clusters, absorption of even a single IR photon is expected to increase the rate for the loss of a water molecule from the size-selected precursor ions under these conditions, although absorption of multiple IR photons can also occur. Because multiple laser pulses are used, product ions are also exposed to laser photons and may subsequently photodissociate. Precursor sizes and laser irradiation times were carefully selected to ensure that product ions formed by sequential loss of water molecules from a larger cluster did not interfere with a smaller isolated precursor.

Photodissociation rates are determined from the relative abundance of the precursor and product ions and the irradiation time using eq 1:

$$k_{\text{photodissociation}} = -\ln\left\{\frac{[\text{Precursor Ion}]}{[\text{Precursor Ion}] + \sum[\text{Product Ion}]}\right\}/\text{time} \quad (1)$$

Photodissociation rates are corrected for the background BIRD rate and the frequency-dependent laser power using eq 2:

$$\text{intensity} = \frac{k_{\text{photodissociation}} - k_{\text{BIRD}}}{\text{power}\ (\nu)} \quad (2)$$

The resulting photodissociation intensities (s^{-1} W^{-1}) account for sequential dissociation of product ions, irradiation time, background BIRD, and the frequency-dependent laser power.[8,53] Repeating this process as a function of laser frequency yields multiple infrared action spectra that are acquired simultaneously. This method of spectral acquisition has the advantages that relative photodissociation yields of different ions can be accurately compared because the ions experience identical conditions, and the spectra can be efficiently acquired in significantly less time than measuring the spectra individually.[30,62]

One potential complication in the interpretation of action spectra is that photodissociation intensities may differ from experimental linear absorption and calculated spectra. These effects are expected to be minimized under conditions where ambient blackbody dissociation occurs and absorption of a single laser photon is sufficient to increase the dissociation rate. The mass spectra exhibit no particularly intense abundances in the cluster distributions, suggesting the absence of any significant "magic number" effects, and differences in water binding energies for the larger clusters should be small.[1,55,60] Thus, action spectra for the larger clusters are expected to be similar to linear absorption spectra. For the smallest clusters, absorption of a single laser photon may not be adequate to induce dissociation for the fraction of the ion population with the lowest internal energy. However, sequential absorption of multiple photons almost certainly occurs over the course of irradiation by many laser pulses, which may affect band intensities. Therefore, the experimental spectra are referred to as infrared multiple photon dissociation (IRMPD) spectra to reflect contributions from sequential absorption of multiple photons and to emphasize the potential differences between these action spectra and linear absorption spectra. Potential IRMPD effects are expected to be greatest for clusters that bind water molecules the strongest, *i.e.*, the smallest clusters. The role of single versus multiple photon absorption as a function of cluster size, laser fluence, and copper jacket temperature can be elucidated by modeling the radiative absorption, radiative emission, and dissociation processes using a master equation approach.[61]

Infrared Action Spectra. These spectra contain two classes of bands that occur above or below roughly 3550 cm^{-1}. The higher-frequency bands are attributable to the stretches of hydroxyl groups that do not donate a hydrogen bond (free-OH), and these bands have proven to be especially useful for characterizing hydrated ion structure.[7−10,20−22,63] Assignments in this region are made by comparisons with spectra obtained for other ions and calculated absorption spectra. The lower-frequency bands are attributable to the stretches of hydroxyl groups that do donate a hydrogen bond (bonded-OH). Duncan and co-workers report that the most red-shifted bands in the bonded-OH region of hydrated metal ions are attributable to hydroxyl groups that donate a hydrogen bond to an outer-shell, single-acceptor-only water molecule, whereas the less red-shifted bands in the bonded-OH region are attributable to water molecules that accept and donate additional hydrogen bonds and are involved in hydrogen-bonding networks.[7] However, assigning bands in the bonded-OH region to specific hydrogen-bonding motifs is extremely challenging because of the large number of candidate structures, increasing spectral congestion with increasing cluster size,[20] and finite temperature effects.[23]

Structures of $M^{2+}(H_2O)_6$. The spectra for $M^{2+}(H_2O)_6$ (M = Mg and Ba) are shown in Figure 1. These spectra have only two bands and are qualitatively similar to those reported previously for $Ag^+(H_2O)_3$,[16] $Ca^{2+}(H_2O)_{4-6}$,[8] $K^+(H_2O)_3$,[4] and $Ni^+(H_2O)_3$,[7] which adopt structures in which all water molecules coordinate directly with the metal ion and form no interwater hydrogen bonds. Using assignments made for those ions, these

(56) Ross, R. B.; Powers, J. M.; Atashroo, T.; Ermler, W. C.; Lajohn, L. A.; Christiansen, P. A. *J. Chem. Phys.* **1990**, *93*, 6654–6670.
(57) Zhao, Y.; Truhlar, D. G. *Theor. Chem. Acc.* **2008**, *120*, 215–241.
(58) Lee, M. S.; Maslen, P. E.; Head-Gordon, M. *J. Chem. Phys.* **2000**, *112*, 3592–3601.
(59) Shao, Y.; et al. *Phys. Chem. Chem. Phys.* **2006**, *8*, 3172–3191.
(60) Donald, W. A.; Williams, E. R. *J. Phys. Chem. A* **2008**, *112*, 3515–3522.
(61) Price, W. D.; Schnier, P. D.; Jockusch, R. A.; Strittmatter, E. F.; Williams, E. R. *J. Am. Chem. Soc.* **1996**, *118*, 10640–10644.
(62) Oomens, J.; Polfer, N.; Moore, D. T.; van der Meer, L.; Marshall, A. G.; Eyler, J. R.; Meijer, G.; von Helden, G. *Phys. Chem. Chem. Phys.* **2005**, *7*, 1345–1348.
(63) Bush, M. F.; Prell, J. S.; Saykally, R. J.; Williams, E. R. *J. Am. Chem. Soc.* **2007**, *129*, 13544–13553.

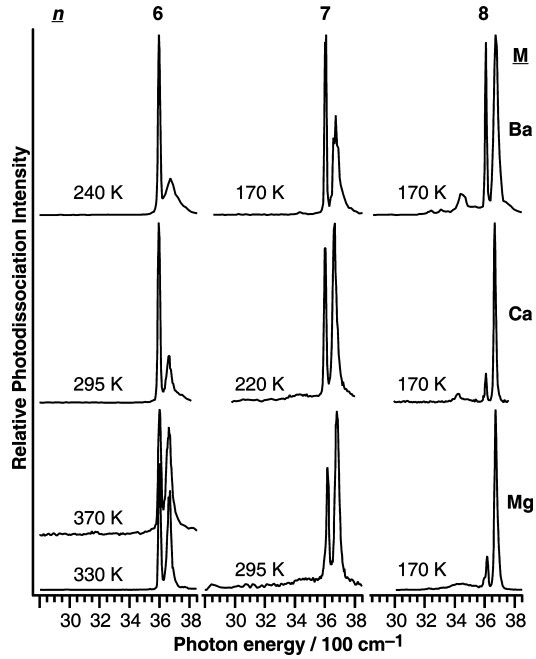

Figure 1. IRMPD spectra of $M^{2+}(H_2O)_{6-8}$ (M = Mg, Ca, and Ba). Copper jacket temperatures are labeled on each spectrum. The spectra for M = $Ca^{2+}(H_2O)_n$ and $Ba^{2+}(H_2O)_7$ have been reported previously.[8]

bands are assigned to the symmetric (ν_{sym}) and asymmetric (ν_{asym}) stretches of water molecules that interact only with the metal ion. No bonded-OH bands are observed at lower frequency. These results indicate that the CN of the metal ions in these clusters is 6. The ν_{sym} and ν_{asym} of $M^{2+}(H_2O)_6$ are centered near 3600 and 3670 cm^{-1}, respectively, for all M, and are significantly red-shifted from those of an isolated water molecule (3657 and 3756 cm^{-1}, respectively)[64] because of partial electron transfer from the water molecule to the metal.[7,8] The red shift of these bands in the spectra of small hydrated divalent metal ions is greater than that observed for hydrated monovalent metal ions,[8] consistent with increased charge transfer to divalent metal ions relative to monovalent metal ions in bulk aqueous solution.[52]

The IRMPD spectra of $Mg^{2+}(H_2O)_6$ measured at copper jacket temperatures of 330 and 370 K are very similar and exhibit only small differences in the width of the ν_{asym} band; the greater width of that band in the latter spectrum is consistent with the population of higher internal rotational states at the higher copper jacket temperature.[65] These spectra are consistent with structures in which all water molecules directly solvate the metal ion at both temperatures. In contrast, evidence for two different structures of $Mg^{2+}(H_2O)_6$ was reported from BIRD studies at these two temperatures based on trends in the dissociation kinetics.[2,32] Threshold dissociation energies (E_0) for the loss of a water molecule of 98 and 88 kJ/mol at the lower and higher temperatures, respectively, were obtained by fitting the slopes of the Arrhenius data in combination with master equation modeling.[32] The binding energy of water to $Mg^{2+}(H_2O)_6$ is higher than that for $Ca^{2+}(H_2O)_6$ at low temperature, as expected because of the smaller ion size, but the opposite is true at higher temperature. Here, the BIRD rate for the loss of one water molecule from M = Ca (0.00176 ± 0.00004 s^{-1}) is greater than

(64) Fraley, P. E.; Rao, K. N. *J. Mol. Spectrosc.* **1969**, *29*, 348–364.
(65) Vaden, T. D.; Lisy, J. M.; Carnegie, P. D.; Pillai, E. D.; Duncan, M. A. *Phys. Chem. Chem. Phys.* **2006**, *8*, 3078–3082.

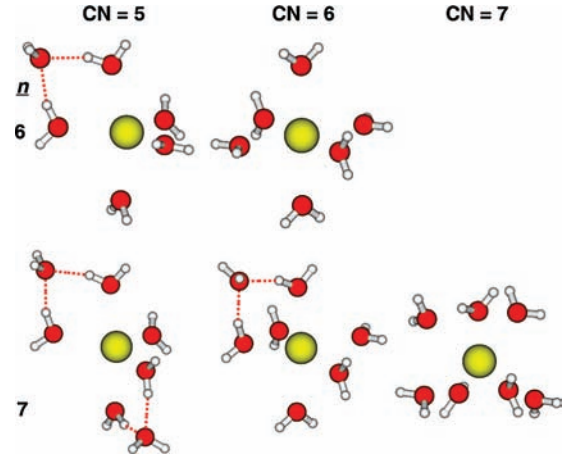

Figure 2. B3LYP/6-311++G(2d,2p) electronic energy-minimized structures of $Ba^{2+}(H_2O)_n$ (n = 6 and 7) that have coordination numbers ranging from 5 to 7.

that for M = Mg (0.00152 ± 0.00001 s^{-1}) at 330 K, whereas the rate for M = Mg (0.039 ± 0.001 s^{-1}) is greater than that for M = Ca (0.0310 ± 0.0009 s^{-1}) at 370 K, consistent with the earlier report. The similarity of the IRMPD spectra of $Mg^{2+}(H_2O)_6$ at the two different temperatures indicates that any structural differences between isomers that may be present are subtle and are not reflected by the IRMPD spectra.

Onset of Second Hydration Shell Formation. The IRMPD spectra of $M^{2+}(H_2O)_7$ (M = Mg, Ca, and Ba) all exhibit differences from those for $M^{2+}(H_2O)_6$. There is photodissociation, albeit weak, at frequencies below 3520 cm^{-1} that is not observed in the spectra of the smaller clusters. These lower-frequency bands for the larger clusters share similarities with those observed for $H^+(H_2O)_{n>2}$,[13,20,21] $K^+(H_2O)_{n>3}$,[4] and $Ni^+(H_2O)_{n>3}$,[7] which all adopt structures with hydrogen bonding between water molecules. The presence of additional lower-frequency bands for clusters with interwater hydrogen bonding is also supported by comparisons between absorption spectra calculated for candidate structures that have different coordination numbers (Figures 2 and 3; data for Ba shown). The structures with CN values of 5 and 6 have double-acceptor water molecules in the second shell (Figure 3) and are calculated to absorb strongly near 3400 cm^{-1}. Structures with single-acceptor water molecules in the second shell are also low in energy and are calculated to also absorb at even lower frequencies.[8]

The broad photodissociation observed from roughly 3000 to 3500 cm^{-1} in the spectra of $Mg^{2+}(H_2O)_7$ and $Ca^{2+}(H_2O)_7$ is consistent with the presence of populations of structures containing either a single-acceptor or a double-acceptor water molecule in the second shell. The spectrum of $Ba^{2+}(H_2O)_7$ has a very weak band at 3430 cm^{-1} that is consistent with a small population of ions that have a double-acceptor water molecule in the second shell.

The relative intensities of the bands near 3600 and 3670 cm^{-1} depend on metal ion identity and provide a complementary signature for the extent of second-shell formation. In the CN = 7 structure, these bands are assigned to the free ν_{sym} and ν_{asym} of the acceptor-only water molecules that only interact with the metal ion. In the CN = 5 and 6 structures, the hydrogen bond donors have one hydroxyl stretch that is red-shifted to lower frequency, and the other hydroxyl stretch (free-OH) is superimposed on the ν_{asym} bands for the water molecules that do not donate a hydrogen bond. Therefore, the band near 3600 cm^{-1}

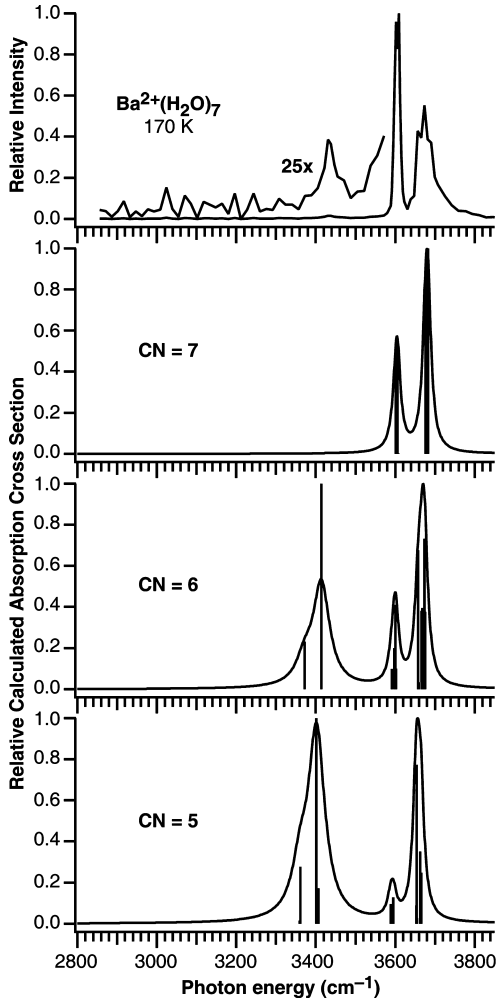

Figure 3. IRMPD spectrum of $Ba^{2+}(H_2O)_7$ (reported previously)[8] and the calculated absorption spectra of three candidate structures at the B3LYP/6-311++G(2d,2p) level of theory. Calculated harmonic vibrational frequencies have been scaled by 0.953.

is preferentially depleted when inner-shell water molecules donate hydrogen bonds to the second solvent shell. This effect is clearly illustrated in the calculated spectra for $Ba^{2+}(H_2O)_7$ in Figure 3; the relative intensity of the band near 3600 cm^{-1} increases with increasing coordination number. In the IRMPD spectra of $M^{2+}(H_2O)_7$, the relative intensity of this band increases with increasing metal ion size. Both the relative photodissociation intensity below 3550 cm^{-1} and the relative integrated intensities of the two high-frequency bands indicate that the average CN of Ba in $M^{2+}(H_2O)_7$ is higher than that of either Ca or Mg.

The relative intensities of the two highest-frequency bands in the spectra of $Mg^{2+}(H_2O)_8$ and $Ca^{2+}(H_2O)_8$ are nearly identical. The photodissociation in the bonded-OH region is centered near 3450 cm^{-1} and is very weak below 3300 cm^{-1} in both spectra, although the relative photodissociation intensity in this region is less for $Ca^{2+}(H_2O)_8$. These results suggest that second-shell water molecules in these ions predominantly accept two hydrogen bonds and that these ions may have similar structures. The relative intensity of the band near 3600 cm^{-1} is substantially greater for $Ba^{2+}(H_2O)_8$ than that for the other two ions, suggesting that the average CN value of Ba in $M^{2+}(H_2O)_8$ is greater than those for M = Mg and Ca, consistent with results for $M^{2+}(H_2O)_7$.

Intensities in the bonded-OH regions of these spectra are very weak relative to the free-OH bands when compared to the calculations (Figure 3) and to experimental spectra of hydrated monovalent ions.[4,6,7,13] Weak intensities in the bonded-OH regions may be due to contributions of higher CN structures that do not have bonded-OH bands, but other factors may also contribute. Because the threshold dissociation energies for the loss of one water molecule from these ions (values for $Mg^{2+}(H_2O)_6$ and $Ca^{2+}(H_2O)_6$ are ~88−98 kJ/mol)[2] are even greater than that for $H^+(H_2O)_3$ (81 kJ/mol),[33] photodissociation of these small cluster ions will be enhanced by the absorption of multiple laser-generated photons. Because the bonded-OH region is at lower frequency than the free-OH region, on average, more photons are required to dissociate the cluster in the former region, so the intensity of these bands will be lower. These effects should be less for larger clusters of hydrated divalent metal ions, for which water binding energies will rapidly approach those of hydrated monovalent ions.[60]

Comparisons with Theory. The B3LYP hybrid density functional is often used for ionic clusters of this size, but results from Rotzinger indicate that approach may not correctly balance metal−ligand and ligand−ligand interactions for hydrated multiply charged ions.[66] Therefore, we performed calculations at the B3LYP level of theory and calculated single-point energies using alternative methods that have more accurate treatments of electron correlation. Structures of $M^{2+}(H_2O)_{6-7}$ (M = Mg, Ca, and Ba) with CN values ranging from 5 to 7 were investigated computationally to further understand the experimental data and to evaluate the computational methods.

The low-energy structures of these ions were similar for all M, except the CN = 7 structure was not stable for M = Mg and energy minimized to a CN = 6 structure, consistent with recent results reported by Tunell and Lim.[35] Representative structures for M = Ba are shown in Figure 2. Relative free energies at 298 K for these structures were calculated at the B3LYP/6-311++G(2d,2p) (B3LYP), M06//B3LYP/6-311++G(2d,2p) (M06), and TRIM-MP2//B3LYP/6-311++G(2d,2p) (TRIM-MP2) levels of theory and are shown in Figure 4. Free energies at 0 K and at the temperature of the copper jacket for the relevant experiment are reported in the Supporting Information (Table 1). The M06 and TRIM calculated free energies use thermodynamic corrections determined using harmonic vibrational frequencies calculated at the B3LYP/6-311++G(2d,2p) level of theory. Uncertainties associated with using harmonic frequencies to calculate free energies, particularly for clusters that have many low-frequency vibrational modes, are not well characterized.

All three levels of theory indicate that the CN of M in $M^{2+}(H_2O)_6$ is 6 for all M. At the B3LYP level of theory and 298 K, the CN = 5 structure is 3 and 14 kJ/mol higher in free energy for Mg and Ca, respectively, whereas that structure is ~16 and 25 kJ/mol higher in free energy for Mg and Ca, respectively, at both the M06 and TRIM-MP2 levels of theory. These results are consistent with many previous computational studies indicating that six-coordinate structures are lowest in energy for $Mg^{2+}(H_2O)_6$[32,67,68] and $Ca^{2+}(H_2O)_6$.[3,8,36,67,68] The CN = 5 structure is 1−4 kJ/mol higher in free energy at 298 K than the CN = 6 structure for Ba at all levels of theory.

(66) Rotzinger, F. P. *J. Phys. Chem. B* **2005**, *109*, 1510–1527.
(67) Pavlov, M.; Siegbahn, P. E. M.; Sandström, M. *J. Phys. Chem. A* **1998**, *102*, 219–228.
(68) Merrill, G. N.; Webb, S. P.; Bivin, D. B. *J. Phys. Chem. A* **2003**, *107*, 386–396.

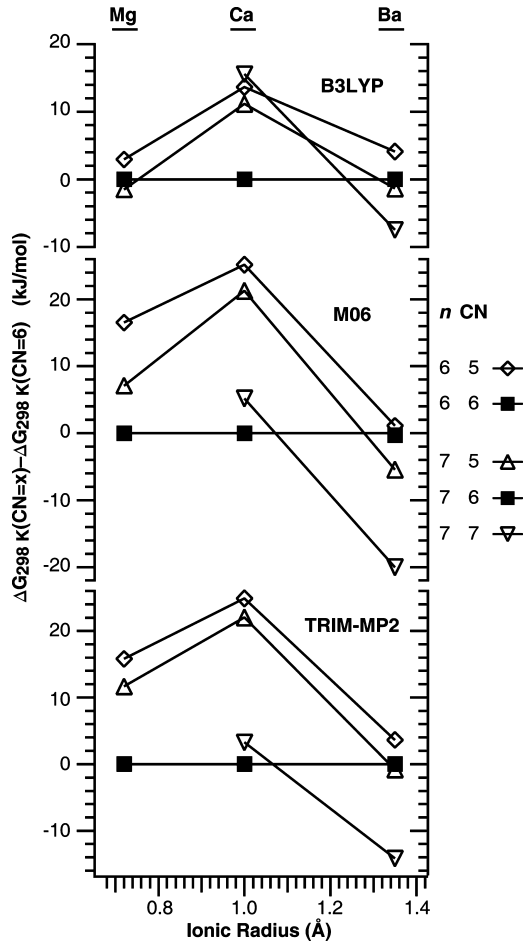

Figure 4. Relative 298 K free energies of structures that have different coordination numbers for $M^{2+}(H_2O)_{6-7}$ (M = Mg, Ca, and Ba) at the B3LYP/6-311++G(2d,2p), M06//B3LYP/6-311++G(2d,2p), and TRIM-MP2//B3LYP/6-311++G(2d,2p) levels of theory. CN = 7 structures are not stable for $Mg^{2+}(H_2O)_7$.

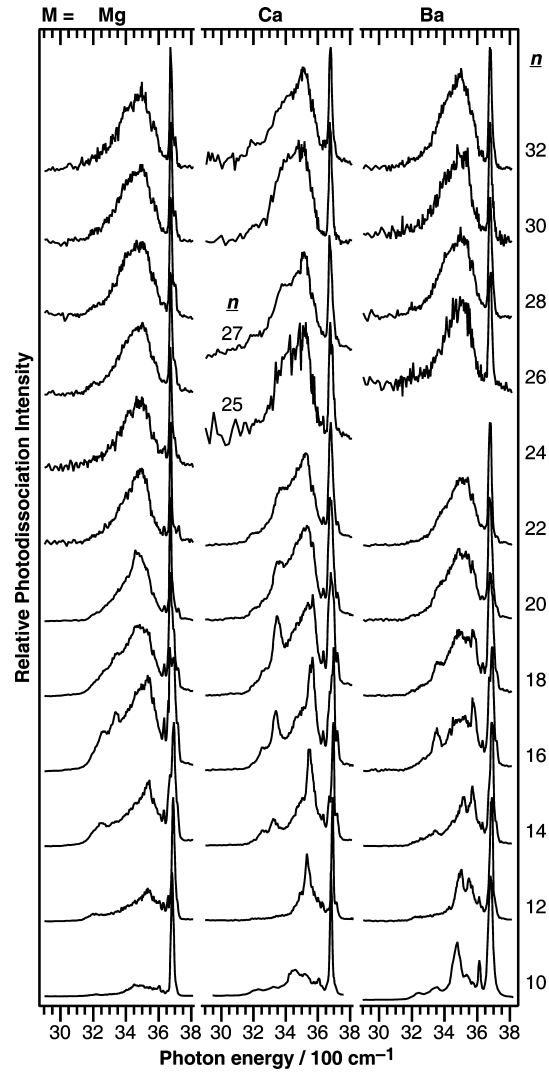

Figure 5. IRMPD spectra of selected $M^{2+}(H_2O)_n$ clusters measured at a copper jacket temperature of 130 K (150 K for $Ca^{2+}(H_2O)_{10}$). Spectra for M = Ca have been reported previously.[8,30]

The B3LYP calculations indicate that the CN values of M in $M^{2+}(H_2O)_7$ are 5, 6, and 7 for M = Mg, Ca, and Ba, respectively, at 298 K. For M = Mg, the CN = 6 structure is only 1 kJ/mol higher in free energy. For M = Ca, the CN = 7 structure is 16 kJ/mol higher in free energy. Interestingly, B3LYP/6-311++G(3df,3pd)//6-31G(d,p) calculations by Tunell and Lim[35] and B3LYP/6-311++G(2d,2p)//6-311+G(d,p) calculations by Armentrout and co-workers[3] indicate that CN = 7 structures are 16 and 22 kJ/mol higher in free energy, respectively, than the CN = 6 structure. Part of the discrepancy with the results from Armentrout and co-workers[3] can be attributed to the identification of a somewhat different CN = 7 structure here that, depending on the level of theory, is 4−7 kJ/mol lower in energy.

The M06 and TRIM-MP2 levels of theory yield remarkably similar results for all structures. For $M^{2+}(H_2O)_7$, the CN = 6 structure is lowest in free energy at 298 K for M = Mg, the CN = 6 and CN = 7 structures are very close in free energy for M = Ca, and the CN = 7 structure is lowest in free energy for M = Ba. Structures with higher CN values are favored at the M06 and TRIM-MP2 levels of theory compared to those at the B3LYP level of theory (Figure 4).

The IRMPD spectrum of $Ba^{2+}(H_2O)_7$ indicates the presence of populations of both the CN = 6 and CN = 7 structures, and a small population of CN = 7 structures could be present for both $Ca^{2+}(H_2O)_7$ and $Mg^{2+}(H_2O)_7$ as well. For $Ca^{2+}(H_2O)_7$, the M06 and TRIM-MP2 calculations indicate that these structures are close in free energy (+6 and +4 kJ/mol, respectively, at 170 K), whereas the B3LYP calculations suggest that the CN = 7 structure should not be significantly populated under these conditions (+16 kJ/mol at 170 K). The presence of a very weak signature for a double-acceptor water molecule in the IRMPD spectrum of $Ba^{2+}(H_2O)_7$ indicates some fraction of the population must have CN < 7, but it is difficult to ascertain accurate relative abundances for the structures that contribute to the experimental spectrum. The B3LYP calculations indicate that all three structures of $Ba^{2+}(H_2O)_7$ are within 1 kJ/mol of free energy at 170 K, whereas the M06 and TRIM-MP2 calculations indicate that structures with smaller coordination numbers are at least 7 kJ/mol higher in free energy.

Infrared Action Spectra of Larger Clusters. Infrared action spectra were measured for selected *n* ranging from 10 to 32 for $M^{2+}(H_2O)_n$ (M = Mg and Ba) (Figure 5). These spectra exhibit many bands that persist and evolve with increasing *n* and share many similarities with those reported previously for M = Ca,[8,30] and a selection of those spectra are also shown Figure 5 for comparison. The bonded-OH regions of these spectra, although highly congested, have large integrated intensities and exhibit

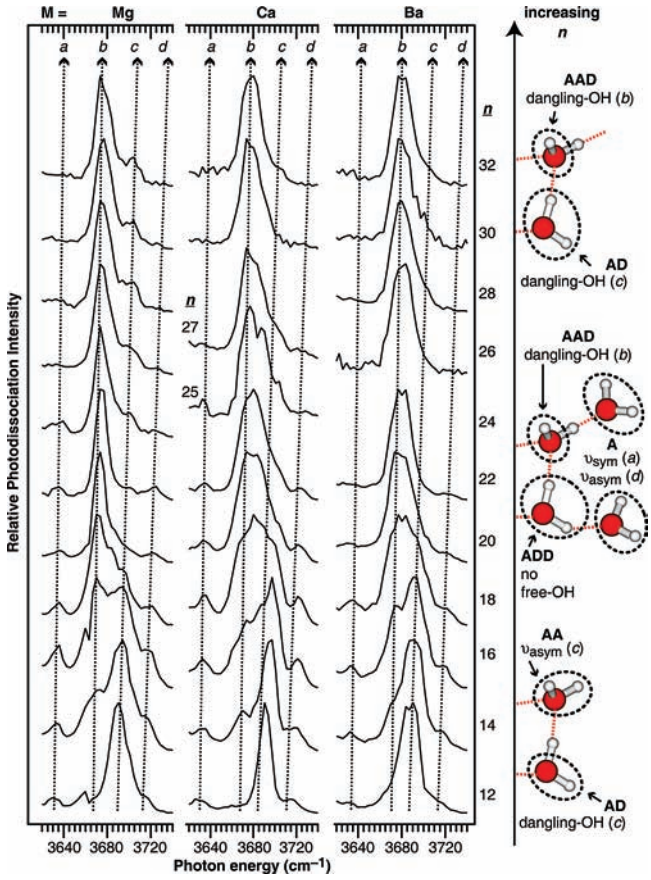

Figure 6. IRMPD spectra of selected $M^{2+}(H_2O)_n$ clusters in the free-OH region measured at a copper jacket temperature of 130 K. Spectra for M = Ca have been reported previously.[30]

many similarities with spectra of large protonated water clusters.[20−22] The free-OH regions of these spectra exhibit multiple resolved bands and reveal detailed structural information.

The free-OH regions of these spectra are shown in Figure 6 and contain up to four bands, similar to those observed previously for many hydrated ions, including $H^+(H_2O)_n$,[20,22,27] $Cu^{2+}(H_2O)_n$,[9] and $M^{3+}(H_2O)_n$ (M = rare earth metal).[31] These bands for $M^{2+}(H_2O)_n$ are denoted *a*−*d* using the notation of Shin et al.[20] These bands for $H^+(H_2O)_n$ have been assigned to the free-OH stretches of water molecules in different hydrogen-bonding configurations,[20,22,27] which are shown schematically in Figure 6. Acceptor water molecules either accept a hydrogen bond from another water molecule or interact directly with the metal ion, and donor water molecules donate a hydrogen bond to another water molecule. Bands *a* and *d* are assigned to ν_{sym} and ν_{asym} of single-acceptor-only water molecules (**A**, one-coordinate water), respectively. Band *b* is assigned to the dangling-OH stretches of double-acceptor, single-donor water molecules (**AAD**, three-coordinate water).[20,22] Band *c* is assigned to both the dangling-OH stretches of single-acceptor, single-donor (**AD**) water molecules[20,22] and the asymmetric stretches of **AA** water molecules,[8] which are both two-coordinate motifs.

The most intense band in the spectra of $M^{2+}(H_2O)_{12}$ for all M is *c*, which indicates that two-coordinate hydrogen bonding motifs, such as **AA** and **AD** water molecules, are predominant. With increasing *n*, the intensity of band *c* decreases relative to those of the other bands. The increasing relative intensities of bands *a*, *b*, and *d* relative to band *c* is most consistent with the formation of additional one- and three-coordinate water molecule binding motifs. For example, if an **AD** water molecule forms a new hydrogen bond to a free water molecule, the former would adopt an **ADD** configuration and exhibit no free-OH bands (band *c* depleted), whereas the latter would adopt an **A** configuration and exhibit bands *a* and *d* (Figure 6). Alternatively, if an **AA** water molecule forms a new hydrogen bond to a free water molecule, the former would adopt an **AAD** configuration and exhibit band *b* (band *c* depleted), whereas the latter would adopt an **A** configuration and exhibit bands *a* and *d* (Figure 6).

The relative intensities of bands *b* and *c* for a given *n* are very similar for M = Ca and Ba, whereas those for M = Mg appear most similar to those of slightly larger M = Ca and Ba ions. For example, the relative intensities of bands *b* and *c* are essentially equal at $n \approx 16$ for M = Mg and $n \approx 18$ for M = Ca and Ba. These results are consistent with the CN of Mg being slightly smaller than those of Ca and Ba in these larger hydrated ions, which is consistent with results for smaller hydrated ions (*vide supra*) and condensed-phase experiments.[37]

The relative intensities of bands *a* and *d*, which are spectral signatures for **A** water molecules, monotonically increase until $n \approx 16$, 18, and 18 for M = Mg, Ca, and Ba, respectively, but then decrease with increasing *n* until becoming essentially depleted by $n \approx 30$. The relative intensities of bands *a* and *d* decrease with increasing metal ion size. This indicates that one-coordinate water molecules are most favorable for M = Mg, which is attributable to strong water binding to Mg, causing a greater disruption to the hydrogen-bonding network of water. In contrast, water binding to Ba is much weaker, and it is favorable for water molecules to form additional hydrogen bonds.

Over the size range in which the relative populations of **A** water molecules depend most strongly on M, the bonded-OH regions of these spectra also exhibit their greatest dependence on metal ion identity. In contrast, differences in the relative intensity of the most intense free-OH bands, *b* and *c*, for a given *n* are very subtle for these ions. This result is consistent with the frequency of bonded-OH bands being more sensitive than the free-OH bands to differences in hydrogen-bonding partners. For example, the free-OH bands for all **AAD** water molecules are superimposed, but it is likely that the bonded-OH band for an **AAD** water molecule that donates a hydrogen bond to an **A** water molecule differs significantly from that for a molecule that donates a hydrogen bond to an **AD** water molecule. More sophisticated methods of simulating and characterizing the infrared spectra of larger hydrated clusters in the bonded-OH region are clearly needed.

The bonded-OH regions of these spectra for $n \geq 28$ are very similar for all M. This suggests the structures of these ions depend more strongly on intrinsic water interactions than specific ion−water interactions. The bonded-OH regions of these spectra are considerably blue-shifted from those of bulk water at room temperature, but the bonded-OH spectra of even larger $Ca^{2+}(H_2O)_n$ more closely resemble the condensed-phase spectrum.[30] Increased absorption at higher frequencies in the bonded-OH region of condensed-phase spectra are often attributed to more distorted water structures,[25,26] but some aspects of that interpretation have been challenged recently.[69]

Interestingly, band *c* in the spectra of the largest $Mg^{2+}(H_2O)_n$ clusters is better resolved and slightly more intense than the

(69) Smith, J. D.; Saykally, R. J.; Geissler, P. L. *J. Am. Chem. Soc.* **2007**, *129*, 13847–13856.

corresponding bands in $Ca^{2+}(H_2O)_n$ and $Ba^{2+}(H_2O)_n$. This suggests that some subtle effects of the smaller metal ion on surface water structure persist at this cluster size and that spectra of even larger $Mg^{2+}(H_2O)_n$ should provide an interesting comparison with spectra reported previously for $Ca^{2+}(H_2O)_n$ in that size range.[30]

Conclusions

IRMPD spectra of $M^{2+}(H_2O)_n$ (M = Mg, Ca, and Ba) provide information about differences in the coordination of water to these metal ions. For $M^{2+}(H_2O)_6$, the CN is 6 for all M. For $M^{2+}(H_2O)_7$, clear evidence for the onset of second shell formation for all three metal ions is indicated from both the presence of bonded-OH bands and the relative intensities of the free-OH stretches, but the extent to which higher CN structures are populated depends on metal ion size; evidence for both CN = 6 and 7 structures is indicated for Ba, and both Ca and Mg may have smaller populations of CN = 7 structures as well. These results generally follow trends predicted by theory, although no one level of theory accurately accounts for all the experimental results, and clearly illustrate the benefits of comparing spectra as a function of cluster and metal ion size to assist in interpretation of IRMPD spectra of solvated ion clusters. These results also indicate that the CN of clusters in this size range is more complicated than previously appreciated owing to the presence of multiple structures. The relative stabilities of different structures could, in principle, be obtained by measuring the IRMPD spectra as a function of temperature.

For the intermediate-size clusters, the relative abundance of single-acceptor water molecules for a given cluster size decreases with increasing metal ion size. This indicates that the tighter water binding to smaller metal ions disrupts the hydrogen bond network to a greater extent, resulting in fewer net hydrogen bonds. The spectra of the largest clusters (n = 32) are very similar for Ca and Ba. The free-OH regions of these spectra indicate that most of the surface water molecules accept two hydrogen bonds and donate one hydrogen bond and are thus optimally hydrogen-bonded for surface water molecules. This suggests that intrinsic water properties are more important to the surface structures of these clusters than metal−water interactions by this size. The majority of the surface water molecules in the spectra of the largest M = Mg clusters are also optimally hydrogen-bonded, but some fraction of these surface water molecules only accept one hydrogen bond and donate another, indicating that the subtle effects of this smaller metal ion propagate to the surface structure of water even for clusters containing several solvent shells.

Acknowledgment. The authors thank Prof. Alan G. Marshall and Dr. Gregory T. Blakney (National High Magnetic Field Laboratory) for the loan of, assistance with, and support for the modular FT/ICR data acquisition system (MIDAS) used in these studies and Damon R. Carl for providing coordinates for $Ca^{2+}(H_2O)_7$. Financial support was provided by National Science Foundation grants CHE-0718790 (E.R.W.) and CHE-0650950 (R.J.S.).

Supporting Information Available: Complete ref 59 and Table 1. This material is available free of charge via the Internet at http://pubs.acs.org.

JA901011X